Journal of Structural Geology, Vol. 14, No. 6, pp. 701 to 712, 1992
Printed in Great Britain

0191-8141/92 $05.00+0.00

Populations of faults and fault displacements and their effects on estimates of fault-related regional extension

J. J. WALSH and J. WATTERSON

Department of Earth Sciences, University of Liverpool, P.O. Box 147, Liverpool L69 3BX, U.K.

(*Received* 5 *October* 1989; *accepted in revised form* 15 *January* 1992)

Abstract—Measured populations of fault displacements, derived from regional seismic, oilfield seismic, coalmine plans and outcrop data show a power law distribution with exponents ($-S$) of -0.45 to -0.95 for single-line samples across an array of faults. The more negative values indicate relatively larger numbers of smaller faults. An expression for a population of active faults, derived from the Gutenberg–Richter magnitude–frequency relation for earthquakes, is $\log N = a - b_D \log D$, where D = maximum displacement of a fault, N = number of faults of maximum displacement D or greater, and $b_D \cong 1.0$ and has the same value as b for the corresponding earthquake population. Populations of 'dead' faults existing at the end of a tectonic episode have been numerically derived, using a fault growth model, and satisfy the relation $\log N = a - E \log D$, where E has a value between 1.6 and 2.0. Numerically derived populations of fault displacements in a dead fault population have slopes of $-S$ where $S \cong E - 1$. The contribution of an individual fault to the regional strain varies with the lifetime seismic moment of the fault and is proportional to D^2. Estimation of fault-related extension by summing heaves on faults of a limited size range is valid only if the measured size range of faults accommodates most of the extension. Correction can be made if the S value of the fault displacement population is known.

NOMENCLATURE

A	area of a fault surface
b	negative of slope of earthquake population curve
b_D	negative of slope of active fault population curve
E	negative of slope of dead fault population curve
S	negative of slope of fault displacement population curve
c	variable dependent on material properties
d	cumulative displacement at a point on a fault surface
D	maximum cumulative displacement on a fault
k	ratio u/w for active intraplate faults = $ca\ 6 \times 10^{-5}$
m	earthquake magnitude (unspecified)
M_0	seismic moment
$\mathbf{M}_0$	rate of seismic moment
ΣM_0	sum of seismic moments of a group of faults
M_{0L}	lifetime seismic moment of a single fault or part of fault surface
ΣM_{0L}	sum of lifetime seismic moments of group of faults or fault surfaces
n	exponent of width (W) in displacement–width expression, $D = cW^n$
N	cumulative number of earthquakes/faults/displacements
r	fault surface radius = $W/2$
w	maximum dimension of slip surface in a single earthquake event
W	maximum dimension of fault surface
u	mean slip on slip surface in a single earthquake event
μ	shear modulus

INTRODUCTION

EARTHQUAKE populations have long been known to have systematic size distributions (Gutenberg & Richter 1954, King 1983). Evidence for a systematic size distribution in populations of ancient, or 'dead', faults is more recent (Kakimi 1980, Villemin & Sunwoo 1987, Childs *et al.* 1990, Heffer & Bevan 1990, Marrett & Allmendinger 1990). We take this new evidence as a starting point for investigating possible relationships between the two types of population, each of which is fractal over wide ranges of magnitude and size, respectively. A crucial question is how, if at all, the fractal dimension of each population is related to the fractal dimension of the other.

A systematic relationship between the magnitude of an earthquake and the size of the fault on which it occurs is the basis of the concept of the 'characteristic' earthquake (Schwartz *et al.* 1981, Schwartz & Coppersmith 1984) or the maximum magnitude model (Wesnousky *et al.* 1983). The contrasting b-value model (Wesnousky *et al.* 1983) assumes that slip over the entire surface of a fault is accomplished in several separate slip events giving rise to earthquakes spanning a range of magnitudes, the magnitude of each being a function of the fracture area over which slip occurs in each event and not that of the whole fracture. The implication of the characteristic earthquake model is that the earthquake population deriving from a rock volume is a simple function of the size population of active fractures in that volume. The implication of the b-value model is that the earthquake population is either not a function of the active fracture population or is some complex function of that population: some relationship between earthquake and active fracture populations is likely, if only because big earthquakes result from slip on big fractures. Also in doubt is the relationship between the active fracture population in a seismically active region and the total population of fractures in the region, including those currently inactive.

Support for the characteristic earthquake model derives from a variety of sources. The stratigraphy of scarp-derived colluvium on individual fault segments in the Wasatch and San Andreas fault zones show the slip in successive events to have been relatively constant on each segment (Schwartz & Coppersmith 1984). The predicted moment–frequency distribution, assuming the characteristic earthquake model, for a population of

mapped intraplate Quaternary faults in Japan, of known sizes and slip rates, is virtually identical with that of the 400-year seismicity record (Wesnousky *et al.* 1983). Further support for the characteristic earthquake model is also found in the relationships between maximum dimensions (W) and maximum accumulated displacements (D) on ancient faults and between the mean slip (u) and the slip surface dimension (w) for individual slip events on active faults. D and W are related by

$$D = cW^n, \quad (1)$$

where c = constant and the exponent n is either 2 or 1.5 (Walsh & Watterson 1988, Marrett & Allmendinger 1991). The proposition that $n = 1$ (Scholz & Cowie 1990) is inconsistent with the data presented by either Walsh & Watterson (1988), Scholz & Cowie (1990) or Marrett & Allmendinger (1991). u and w, on the other hand, are linearly related (Scholz 1982, Scholz *et al.* 1986). The two relationships are most easily reconciled if there is both a systematic relationship between u and D and a fault growth model in which w and W are identical, i.e. the characteristic earthquake model. The value of n will be taken as 2, but taking the value as 1.5 would result in no major change to the conclusions. The fault growth model predicts that as W increases throughout the active life of a fault, the earthquake magnitude which is characteristic of the fault will also gradually increase but, in accord with the characteristic earthquake model, the increase will be imperceptible over the time occupied by a few seismic cycles. Observational data on neotectonic faults are limited to a small number of seismic cycles. In the following, for calculation of 'dead' fault and fault displacement populations, this modified characteristic earthquake model is assumed to be valid. Comparison of predicted populations with measured populations then constitutes a test of the modified characteristic earthquake model.

There are several possible mechanisms which complicate the relationship between active fracture and earthquake populations, although some are significant only on short time scales and do not affect what follows; e.g. coupling of slip events on adjacent fractures (Huang & Turcotte 1990). Models are, however, greatly simplified approximations of the real world and even the use of a concept as straightforward as 'number of faults' requires acceptance of a considerable simplification of the three-dimensional branching and splaying which characterizes a typical fault array.

If the concept of the characteristic earthquake could be demonstrated to be valid over a wide range of magnitudes and fault dimensions, seismic data could be used to provide information on the size and location of active fractures within a volume, which could then be applied to study of the failure process. If, on the other hand, a seismic event represents slip on some unknown fraction of a fracture surface then seismic data have more limited value in the study of faults. Data on the systematics of dead fault populations and of earthquake populations are first reviewed. Populations of dead fault populations are then derived from earthquake populations using two alternative strategies and making some necessary assumptions. The theoretical dead fault populations are then compared with measured populations and the resulting discrepancies lead to a reconsideration of the assumptions. Consideration, from both a theoretical and a practical viewpoint, is then given to measurements of regional strain from dead fault populations.

FAULT DISPLACEMENT POPULATIONS

The problems of measuring and interpreting fault and fault displacement populations have been considered by Childs *et al.* (1990), Heffer & Bevan (1990) and Marrett & Allmendinger (1991). The objective is to derive a quantitative measure of the numbers of faults, classified by 'size', in a given volume. Size of a fault may be assessed either by maximum displacement or by maximum dimensions. Sampling may either be of two-dimensional surfaces, such as maps, or along one-dimensional sampling lines through the rock volume. The two-dimensional samples yield only the maximum displacement on each fault trace, i.e. a population which is not the same as that of the maximum displacement on each fault surface. One-dimensional samples are of displacements recorded at each intersection between the sampling line, or lines, and fault traces on maps or sections. Two-dimensional sampling is subject to truncation and censoring effects (Heffer & Bevan 1990) and is complicated by the requirement to distinguish individual fault traces, which cannot always be done objectively in branching fault systems. By contrast, the measurement of fault displacements along one-dimensional sampling lines can be done objectively but is still subject to truncation effects, i.e. any graphical data set can represent only a limited range of fault size.

We have measured one-dimensional fault displacement populations on data sets covering a wide range of scale from regional seismic (Walsh *et al.* 1991), oilfield seismic data (Childs *et al.* 1990, unpublished work), coalmine plans (Childs *et al.* 1990) to outcrop scale. Single- and multi-line sample fault displacement populations for different fault assemblages are shown in Fig. 1 as log–log plots of cumulative number of displacements (N) vs displacement (d), where N is the number of displacements greater than d. Displacement values span only 1.5–2 orders of magnitude in populations derived from seismic reflection and coalmine data and this limited range of scale is characteristic of most fault data represented on maps or cross-sections. For multi-line samples, one-dimensional population curves characteristically have three distinct segments. The steep right-hand segment of the curve (Fig. 1a) intersects the abscissa at the value of the maximum displacement measured, and the length of this segment measured parallel to the ordinate is usually equal to the number of sample lines in the multi-line sample. For most purposes the right-hand segment can therefore be disregarded as a sampling effect. The central segment of the curve is an almost straight line of variable slope, ranging between

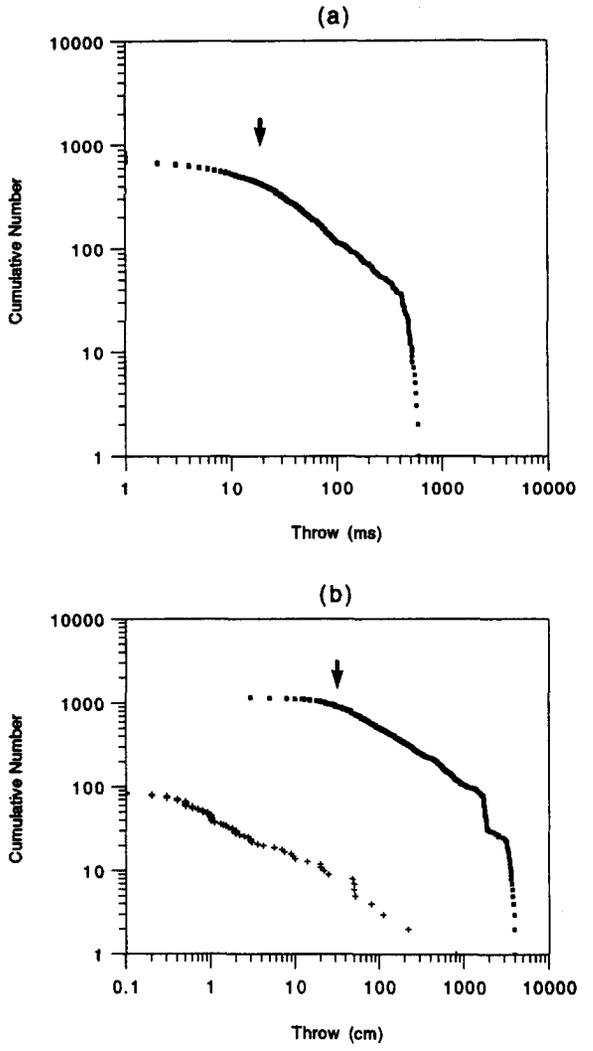

Fig. 1. Fault displacement population curves from seismic reflection, mine plan and outcrop data. (a) Multi-line displacement population curve from seismic reflection data for a single horizon in an offshore oilfield with displacements recorded as throws in ms two-way time (twt). The inferred limit of seismic resolution (arrowed) is *ca* 20 ms and the total length of the sample lines is *ca* 1900 km, with 56 sample lines together covering an area of *ca* 1900 km^2. (b) Multi-line displacement population curve from mine plan data for the Lidgett seam, North Gawber Colliery, Yorkshire (solid squares) and single-line displacement population curve from outcrop data measured in a Carboniferous sandstone–shale quarry in Lancashire, with displacements recorded as throws (cm). The North Gawber dataset is for a *ca* 9 km^2 area which was sampled on 120 lines, each *ca* 3 km long. The lower limit of accurately sampled throws on the coal seam plans is *ca* 30 cm (arrowed). The sample line length of the outcrop dataset is 124 m and the lower limit of accurately measured throws is 1 mm.

−0.45 and −1.2, but for well-constrained data sets is usually between −0.45 and −0.95 (Fig. 1) (Childs *et al.* 1990). The left-hand segment of the curve is shallower than the straight central segment and represents a relatively small number of displacement measurements which are below the limit of resolution of the dataset; for some outcrop datasets, for which displacements can be measured down to 1 mm, there are indications of a real decrease in population slope at scales below which the same power law population may not apply. For the coalmine plan data the limit of resolution is *ca* 30 cm and for the oilfield seismic data set illustrated is *ca* 20 ms two-way time (twt), corresponding to about 30 m displacement (Fig. 1) (Childs *et al.* 1990). The outcrop data are for a single-line sample and give a straight-line population curve from 10 m down to 1 mm, i.e. a range of four orders of magnitude. Our own data and those of others (Villemin & Sunwoo 1987, Heffer & Bevan 1990, Marrett & Allmendinger 1991, Sassi *et al.* in press) show that both one- and two-dimensional populations are fractal. Fault displacement populations are fractal over at least six orders of magnitude (Walsh *et al.* 1991) and are characterized by slopes of −0.45 to −0.95 on plots of log N vs log d, corresponding to fractal dimensions of 0.45–0.95.

POPULATIONS OF EARTHQUAKES AND ACTIVE FAULTS

The magnitude–frequency behaviour of tectonic earthquakes satisfies the empirical relation

$$\log N = a - bm, \qquad (2)$$

where N is the total number of shocks of magnitude m or greater (Gutenberg & Richter 1954). The Gutenberg–Richter (G–R) relationship holds over a wide range of scale and conditions, including laboratory microfracturing studies (Mogi 1962, Scholz 1968) and mining induced fracturing in coalmines (Kusznir *et al.* 1984). The G–R relationship is not expected to hold for a population of seismic events on a single fracture but represents slip events on a population of fractures (Wesnousky *et al.* 1983). The constant a is determined only by the number of events in the sample population but the value b is close to 1.0 and does not usually fall below 0.7 or exceed 1.3 (King 1983). The G–R relationship is valid for the earthquake population of a particular tectonic terrain measured over a certain period, and can be used to characterize the earthquake population within a rock volume for a single seismic cycle. The G–R relationship shows earthquake populations to be fractal over a wide range of magnitudes.

An earthquake population is a simple derivative of the population of active faults only when the following conditions are satisfied.

(1) Active seismic faults are representative of the population of all active faults.

(2) There is a direct relationship between the magnitude of an earthquake and the dimensions of the fault on which it originates, i.e. the modified characteristic earthquake model holds true.

(3) Earthquake recurrence intervals are independent of earthquake magnitudes.

There is no direct indication that the first condition is satisfied but, given that the magnitude–frequency relationship for seismic slip events is highly systematic, there is no obvious reason to suppose that populations of aseismic faults are either less systematic than, or are systematically different from, populations of seismic faults. The second condition is an expression of the modified characteristic earthquake model. The third condition is an untested assumption.

The relationship between the earthquake magnitude (m) and the dimension (w) of the slipped surface can be derived from the moment (M_0)–magnitude relationship (Kanamori & Anderson 1975) which is

$$m \propto C \log M_0, \tag{3}$$

where $C = 1.5$. Hanks & Boore (1984) show that C varies with earthquake magnitude but the effect on what follows is small. By definition

$$M_0 = \mu A u$$

so

$$m \propto 2/3 \log (Au), \tag{4}$$

where μ = shear modulus, A = fault surface area and u = mean slip on the fault. Assuming three-dimensional self similarity, for faults contained wholly within the seismogenic layer

$$Au \propto w^3.$$

From (4)

$$m \propto 2/3 \log w^3$$

so

$$m \propto \log w^2. \tag{5}$$

The relationship between the dimensions of the slipped surface in a single seismic event and the dimensions of the fault on which it occurs is less certain. However, assuming that the characteristic earthquake model is valid for intraplate events, and therefore that individual slip events represent slip over the whole fault surface (Wesnousky *et al.* 1983), the population of active faults can be derived from the earthquake population, assuming that repeat times are the same for individual faults of all sizes. As the dimension of the slipped surface (w) is the same as that of the fault surface (W) then combining (1) and (5)

$$m \propto \log D$$

(if $n = 1.5$ then $m \propto \log D^{1.5}$).

Substituting in (2)

$$\log N = a_D - b_D \log D, \tag{6}$$

where b_D has the same value as b in the G–R relationship (equation 2) and a_D varies with the number of faults in the population. A systematic distribution of fault sizes, as expressed by maximum displacements, is therefore expected in a population of active faults.

In the case of plate boundary or interplate faults, it might be expected that there will not be a relationship between the magnitude of an earthquake and the dimensions of the fault surface on which it originates because individual slip events affect only a part of the plate boundary. However, individual segments of the San Andreas fault system have characteristic earthquakes (Schwartz & Coppersmith 1984) and, in the short term at least, each segment behaves as an isolated single fault (i.e. a single plate boundary fault does not exist). In the longer term the displacements on the different segments must fit together and define a kinematically coherent single unit on the larger scale, in a similar fashion to much smaller scale intraplate fault arrays (Walsh & Watterson 1991).

CALCULATION OF DEAD FAULT POPULATIONS

The population of active faults at any given time is different from the total population of faults existing at the end of a period of faulting. Because an individual fault grows with each successive slip event (Watterson 1986), the active fault population will always include some newly formed faults which are necessary to maintain the G–R relationship as the earlier formed faults grow in size. At any time there must also be a population of inactive faults, if the G–R relationship is maintained for active faults. A relationship between the active and inactive populations at any time can be evaluated if: (a) individual faults grow in a predictable manner; (b) the G–R relationship is maintained with constant b; and (c) some other constraint on the population is introduced. According to the fault growth model (Watterson 1986) W of any fault, and therefore u, increases with each seismic cycle and, assuming a constant b value for the active fault population, the *inactive* fault population can be calculated for any stage during the course of tectonic deformation. When deformation ceases, all faults are inactive and the population is referred to as the *dead* fault population. Two different constraints can be applied in calculating dead fault populations. Both strategies are based on an assumption of constant length of seismic cycles, i.e. constant earthquake recurrence intervals during the life of a fault. Recurrence intervals and their implications are discussed in a later section.

Strategy A

Following this strategy, successive active fault populations are controlled by the size of the largest fault, of which only one is assumed to exist; the size of the largest fault in each successive active fault population is a function of the number of seismic cycles completed (Fig. 2a). A population of active faults satisfying the G–R relationship, with $u/W = 3.16 \times 10^{-5}$ (corresponding to a stress drop of 4.34 bars, Walsh & Watterson 1988) is shown in Table 1. Plots of log N vs log D for calculated populations of all faults (see Appendix 1) are shown in Fig. 3 and satisfy the empirical relation

$$\log N = a - E \log D, \tag{7}$$

where N = total number of faults of maximum displacement D or greater, a varies with the number of faults in the model population and E varies with the b value of the active population, with $E = 1.6$ when $b = 1.0$. The value of E is independent of the number of cycles, Q, if $Q \geq 40$ (see Appendix 1 and Table 2). The distribution of fault sizes, expressed as D, in a dead fault population should therefore be systematic and predictable. This conclusion

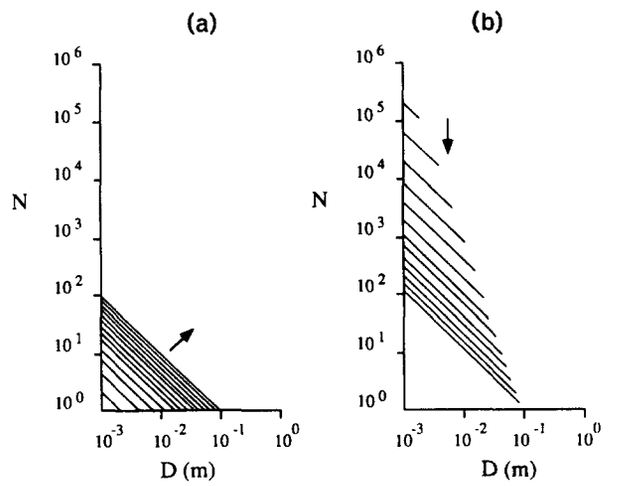

Fig. 2. Log N vs log D curves of successive model active fault populations for (a) Strategy A and (b) Strategy B. An initial fault population of 10^6 faults of 1 mm maximum displacement is used for Strategy B. Successive lines, in directions indicated by arrows, represent active fault populations in successive seismic cycles. Fault growth follows model of Watterson (1986) and growth increment used is 1 mm (see Appendix 1 for details). Strategy A is the single largest fault model and Strategy B assumes a constant rate of seismic moment. In both strategies successive active fault populations are characterized by an increase in D of the largest fault.

is consistent with the data on real fault populations. Strategy A requires an increasing number of faults of the smallest size class to be generated in each cycle to maintain the G–R relationship. The total seismic moment (see below) of each successive active fault population increases throughout the tectonic episode. A constant time-averaged rate of seismic moment would require the length of seismic cycles to increase as the total seismic moment of each cycle increases.

Strategy B

Seismic moment (M_0) is a measure of seismic strain energy (Kostrov 1974) and varies linearly with the rate of fault-related strain of the rock volume, or rate of displacement of terrain boundaries due to seismic faulting. Rate of displacement will be taken as constant. If the rate of displacement of terrain boundaries is constant throughout a tectonic episode then the rate of seismic moment will also be constant, i.e. seismic cycles should have a constant total seismic moment if they are of equal length. For a given initial number of the smallest fault size, successive active fault populations are calculated on the basis of constant seismic moment in each cycle and the maximum fault size is determined by the number of elapsed seismic cycles (Fig. 2b). As with Strategy A, populations of dead faults satisfy equation (7) but values of E are significantly higher (*ca* 3.0) and show little variation. As some of the faults grow larger, because $M_0 \propto W^3$, they account for a rapidly increasing proportion of the total seismic moment, which results in very large numbers of smaller faults becoming inactive rather than growing into larger faults as they would do with Strategy A. The higher death rate of small faults in Strategy B relative to Strategy A leads directly to the higher E values which characterize Strategy B. To maintain the G–R relationship Strategy B requires a decreasing number of active faults of the smallest size class.

A third strategy which could be adopted is to assume that new fractures are generated only at the onset of deformation. As the constant moment model requires generation of relatively few new fractures after the initial fracture generation event, this third option is not considered further.

THEORETICAL FAULT DISPLACEMENT POPULATIONS

The displacement population of a single fault surface can be calculated from an expression (Walsh & Watterson 1987) which shows that the displacement variation is approximately linear from a maximum at the fault centre to zero at the tip-line. The maximum dimension of the fault surface for a given maximum displacement is given by $D = cW^n$, where c varies with rock properties from 2×10^{-7} to $2 \times 10^{-5}\,m^{-1}$ for $n = 2$ (Walsh & Watterson 1988). The displacement population for a single fault is calculated by sampling the displacements at nodes of a square grid on the fault surface and is not affected by the ellipticity of the fault surface. A displacement population for a single fault ($D = 10$ m, $W = 2163$ m, $c = 2.14 \times 10^{-6}$) is shown in Fig. 4.

The fault displacement population for a theoretical fault population is derived by combining the numerically derived numbers of faults in each size class with the numerically derived displacement population for each size of fault. Theoretical fault displacement population curves have characteristic shapes (Fig. 5). The slope of the straight-line segment ($-S$) varies with the chosen b value (equation 2) and, more simply, with the E value of the fault population (equation 7) as shown in Table 3, for

Table 1. Parameters of an active fault population satisfying the Gutenberg–Richter relationship ($b = 1$), with $D/W^2 = 10^{-6}$. D = maximum displacement of smallest fault in each class, z = number of faults in each class, N = number of faults with displacement greater than lower limit of specified class, W = fault maximum dimension. z_i = number of slip events required for smallest faults of one class to grow to the minimum size of the next class (see Appendix 1)

Class	1	2	3	4	5	6	7
D (m)	0.001	0.01	0.1	1.0	10	100	1000
z	90,000	90,000	9000	900	90	9	1
N	1,000,000	100,000	10,000	1000	100	10	1
W (m)	31.62	100	316	1000	3160	10,000	31,600
z_i	2	7	22	70	216	700	2163

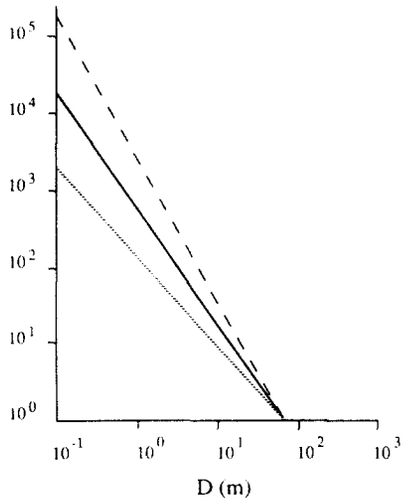

Fig. 3. Log N vs log D curves for dead fault populations derived from active fault populations of varying b_D value, following Strategy A (see text). b_D values for active fault populations are 1.3 (broken line), 1.0 (solid line) and 0.7 (dotted line) and b values are the same for the corresponding earthquake populations if the characteristic earthquake model is valid.

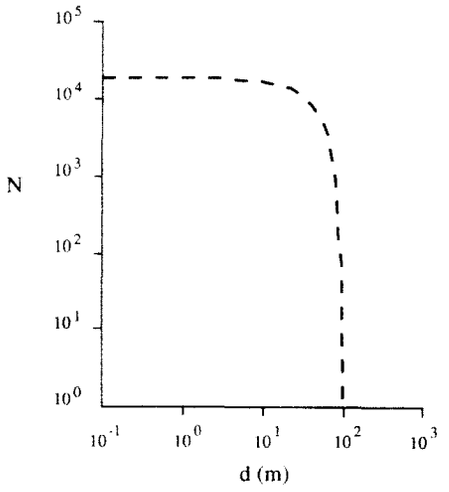

Fig. 4. Log N vs log d curve for a fault of maximum displacement 10 m and $D = cW^2$, where c is 2.137×10^{-6}, a value which is characteristic of faults in rocks of shear modulus (μ) = 10 GPa, i.e. hard sandstone (Walsh & Watterson 1988).

realistic values of E (1.3–2.5), where $S \cong E - 1$. The right-hand segment of the curve is largely a sampling artefact but its form also varies with the largest displacement value, which can be less than the maximum displacement on the largest fault (Fig. 5). The largest displacement value included in the population and the maximum displacement on the largest fault sampled must be separately specified for calculation of a model population, because the largest displacements on the biggest faults may lie outside the sampled volume. The range of curves which could be derived from sampling a single population, with the maximum displacement on the largest fault sampled in each case, is shown in Fig. 6. In practice, the maximum displacement on the largest fault is unlikely to be sampled when only few displacements are included in the sample so only the convex upward curves are of practical interest. The right-hand segment of the population curve steepens with increase in the number of sample lines (Fig. 6) and also when the maximum displacement value sampled is much less than the maximum displacement on the largest fault in the sample (Fig. 5).

Table 2. Populations of dead faults following Strategy A for different values of relevant variables. All populations give straight lines on log N vs log D plots and 40 events are needed to achieve steady-state slopes. Default values of variables (df) are provided below. D = maximum initial fault size (maximum displacement in metres). Q = number of growth events (seismic cycles). b_D = negative of slope of population of active faults which is assumed to be equal to the b value of the G–R relationship for the corresponding earthquake population, (df) = 1.0. u/W = slip/width ratio in each event, (df) = 3.16×10^{-5}. c = constant in $D = cW^2$, (df) = 2.2×10^{-5}. l = minimum fault size (m), (df) = 0.001. E = negative of slope of log N vs log D curve for dead fault population

D	Q	b	u/W	c	l	E
0.3	40	(df)	(df)	(df)	(df)	1.60
0.3	40	0.7	(df)	(df)	(df)	1.30
0.3	40	1.3	(df)	(df)	(df)	1.80
0.3	40	(df)	3.16×10^{-4}	(df)	(df)	1.35
0.3	40	(df)	3.16×10^{-6}	(df)	(df)	1.66
0.3	40	(df)	(df)	2.2×10^{-6}	(df)	1.42
0.3	40	(df)	(df)	2.2×10^{-4}	(df)	1.70
0.3	40	(df)	(df)	(df)	0.01	1.65
0.3	40	(df)	(df)	(df)	0.0001	1.40

COMPARISON OF THEORETICAL AND MEASURED FAULT DISPLACEMENT POPULATIONS

The central and right-hand segments of data and model population curves can be matched by varying, within an acceptable range, the b value of the earthquake population incorporated in the model and by varying the difference between the maximum sized fault

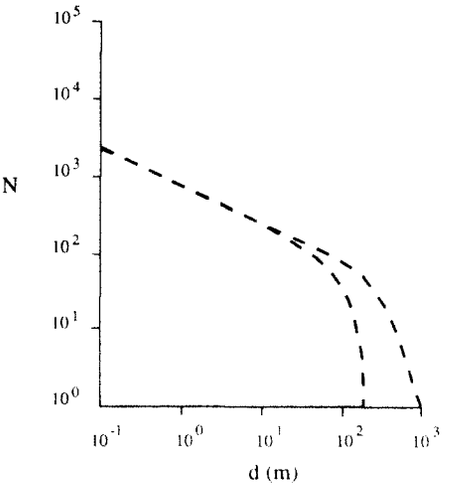

Fig. 5. Numerically derived log N vs log d plots showing the effects of changes in the largest sampled displacement. The maximum displacement of the largest fault in the population is the same in both cases (1000 m). In one case (upper curve), the whole of all the faults in the population is sampled including the maximum displacement on the largest fault. In the other case (lower curve) parts of some of the largest faults are not sampled, i.e. only displacements of less than a given value (200 m) are included. Minimum sampled displacement = 0.1 m, and E = 1.45.

Table 3. E and S values for numerically modelled fault and fault displacement populations

E	S
1.40	0.41
1.50	0.48
1.60	0.60
1.85	0.88
2.00	0.99
2.11	1.11
2.33	1.29

and the maximum displacement reading (see Fig. 5). The slopes ($-S$) of the measured population curves are consistent with derivation from populations with E values of 1.6–2.0, which are consistent with Strategy A but inconsistent with Strategy B. In the measured populations, unusually high slopes are associated with data which span a limited displacement range, i.e. one order of magnitude or less (Childs *et al.* 1990). Some fault displacement population curves derived from published displacement data have slopes equivalent to $E > 2.0$ (Childs *et al.* 1990) but the validity of these high slopes is doubtful.

The similarities between the model-derived and data-derived population curves give some credence to the model and, particularly, to the prediction implicit in equation (10) that populations of dead faults have systematic size distributions. Although the data clearly indicate that the E values for fault populations derived from Strategy A are more realistic than those derived from Strategy B, other consequences of Strategy A give cause for doubt. In particular, the consequence of an increasing total seismic moment with each succeeding seismic cycle is that the regional strain rate also increases, if the recurrence intervals remain constant. A constant rate of seismic moment could be achieved if recurrence intervals increased in proportion to the total seismic moment in each cycle. However, the rate of increase of recurrence interval required to maintain a constant rate of seismic moment with Strategy A is much too great. Increase of maximum fault size from 1 to 100 m would require a 1000-fold increase in recurrence interval, which is not credible.

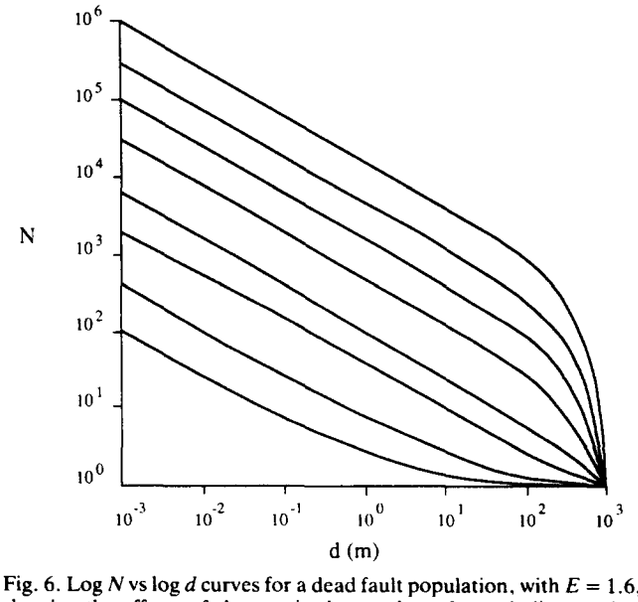

Fig. 6. Log N vs log d curves for a dead fault population, with $E = 1.6$, showing the effects of changes in the number of sample lines and of recorded displacements (N), assuming that the full range of displacements is represented in all samples. This assumption is unlikely to be correct for data with only small numbers of displacement values.

Given the requirement for $E \geq 2$, for recurrence intervals to vary by no more than two orders of magnitude (Scholz *et al.* 1986) and for constant rate of release of seismic moment, no simple relationship between successive active fault populations is evident. Possible sources of error include the absence of data describing the variation, if any, of b value with lithology, strain rate, depth, etc. For example, the b values used in modelling fault populations are not derived from sedimentary basins and it is possible that corresponding values for sedimentary sequences are different. These possible sources of error are, however, unlikely to account for the discrepancies between the numerically-derived and data-derived populations. Strategy B, with constant ΣM_0, is geologically more realistic than Strategy A but gives rise to much higher values of E, or fractal dimension of fault displacements, than are shown by the data.

An obvious possible source of the discrepancy is that the growth model used for numerically deriving the dead fault populations may be wrong. However, the fact that both the numerically-derived and the measured populations are fractal suggests that the growth model used is valid, in general terms if not in detail. The simplest explanation for the discrepancy is that there is not a direct relationship between earthquake b values and the active fracture population, b_D, as has been assumed. To derive realistic E values requires $b_D \leq 0.5$; i.e. significantly less than earthquake b values. Values of $b_D < 1$ would result from one or both of the following possibilities.

(1) The characteristic earthquake model is an oversimplification and individual active fractures host earthquakes of a range of magnitudes.

(2) Earthquake events on a small fracture have shorter recurrence intervals than earthquake events on a large fracture.

In both cases the relative proportions of small earthquakes in an earthquake population exceed the relative proportions of small active fractures in the corresponding fracture population. Whichever of the two possibilities is correct, or if both are correct, there is a strong likelihood that the relationship between b and b_D is systematic. If the discrepancy is due entirely to shorter recurrence intervals for smaller earthquakes then, for $b_D = 0.5$ and $b = 1$, the recurrence interval would vary inversely with D^2, i.e. for each earthquake on a 10 m fault there would be 100 events on a 1 m fault. Such a major difference in recurrence intervals is not supported by location data for microseismic events. A fractal distribution of earthquakes on individual active fractures would appear to be a more likely explanation than major differences of recurrence intervals but recent

indications are that earthquake populations of individual fractures may be log-normal rather than fractal (Scholz 1990). Populations of active fractures are likely to be fractal and, if they are, a simple numerical relationship between b and b_D is probable, but is as yet not known.

FAULT POPULATIONS AND ESTIMATES OF REGIONAL EXTENSION

A recurring observation in extensional terrains is the difference between extension values calculated by summing of observed fault displacements and the much higher values calculated from crustal thinning and basement subsidence studies (Barton & Wood 1983, White *et al.* 1986, Badley *et al.* 1988). Discrepant estimates of basin extension obtained from normal faults are generally resolved by invoking one or a combination of the following explanations. (a) Summation of fault heaves is not an accurate measure of extension (White *et al.* 1986, White 1987, Barnett *et al.* 1987). (b) A large proportion of extension is accommodated by faults too small to be imaged on seismic sections (Angelier & Colletta 1983, Barton & Wood 1983, 1984). (c) Ductile deformation accounts for significant amounts of basin extension (Angelier & Colletta 1983, Barnett *et al.* 1987). This last explanation is the same as (b) if ductile is taken to refer to strain accommodated by discontinuities on a scale below that of the scale of observation, such as fault throws less than 20–30 m for seismic reflection data at depths greater than 2 km (Barnett *et al.* 1987). On the scale of seismic reflection data, ductile and plastic processes cannot be differentiated. (d) Depth-dependent stretching models are applicable to sedimentary basin evolution (Roydon & Keen 1980, Hellinger & Sclater 1983, Badley *et al.* 1988). We restrict our discussions to factors which could be responsible for underestimates of extension in the upper crust and, therefore, for apparent departures from the uniform stretching model (McKenzie 1978).

Although the sum of fault heaves is known not to be a precise measure of fault-related extension (Barnett *et al.* 1987), the consequent relatively small inaccuracy is unlikely to account for the large discrepancies reported. Analysis of theoretical and measured fault populations can be used to estimate the relative importance of small faults in regional extension. The proportion of displacement accommodated by small faults relative to larger faults varies with the slope $(-E)$ of the dead fault population curve. Characteristic E values derived from coalfield and oilfield datasets range from 1.6 to 2. For an E value of 1.6 and a maximum fault size of 2 km, the sum of the maximum displacements on faults between 0.1 and 30 m maximum displacement is *ca* 30 times the sum of maximum displacements on faults between 30 and 2000 m. Similarly the sum of maximum displacements on faults of 100–1000 m maximum displacement is *ca* 18 times that on faults between 1000 and 2000 m. These values do not, however, indicate the relative contributions of these fault size ranges to the regional deformation because the maximum displacement on a fault is not linearly related to its lifetime seismic moment which is a direct measure of the contribution to regional strain.

An estimate of the relative contributions to extension of a region by faults of different size is obtained by summing the lifetime seismic moments on faults of each size in a fault population. For earthquake populations, with typical b values, the contribution of small earthquakes to total seismic energy release is relatively minor (Jackson & McKenzie 1988). The seismic moment of a single earthquake event on a fault is given by:

$$M_0 = umA$$

and so

$$M_0 \cong umW^2.$$

The total seismic moment of a fault (M_{0L}) which grows to a given size during its lifetime is proportional to D^2 (see Appendix 2) and the sum of the lifetime moments (ΣM_{0L}) of different size ranges of faults can be compared using

$$\Sigma M_{0L} \propto (2 \log N)/E \quad \text{(see Appendix 2)}.$$

The relative total seismic moments contributed by all faults of final maximum displacements of different size ranges is shown in Table 4 for a dead fault population with $E = 1.6$ and maximum fault size of 2 km. In this case, the larger faults contribute an overwhelming proportion of the seismic moment and contribute the same proportion to the fault-related regional extension. For populations with E values close to 2, displacements on smaller faults make a significant contribution to the regional strain. In such cases, extension values derived from seismically resolvable displacements will always be underestimates.

An alternative, and more direct, method for assessing the accuracy of fault-related regional extension estimates is to calculate the relative contributions of different displacement values (d) to the total seismic moment,

Table 4. Sum of lifetime moments for different size ranges of faults in populations with different E values ($E \cong S + 1$), expressed as percentage of total lifetime moments of all faults

	Size range D (m)				
E	0.1–1.0	1.0–10	10–100	100–1000	1000–2000
3.0	90.0	9.0	0.9	0.09	0.0009
2.0	22.0	22.0	22.0	22.0	12.0
1.6	2.3	5.7	12.8	39.0	40.2

directly from fault displacement population data. This method is independent of fault growth models and is based on the data-derived populations. A displacement value (d) represents the sum of all the slip events per unit area of the fault surface.

As

$$M_0 = muA$$

the lifetime seismic moment (ΣM_{0L}) is given by

$$\Sigma M_{0L} = mdA$$

so, for unit area of a fault surface characterized by displacement d,

$$\Sigma M_{0L} \propto d$$

and the relative total seismic moments contributed by fault displacements of different size ranges can be calculated from fault displacement population data. The shear modulus is assumed not to vary significantly on the scale of individual faults within the rock volume. Figure 7 shows the proportion of the total lifetime seismic moment, expressed as a percentage of the total fault-related extension, due to fault displacements in given size ranges, for a variety of fault populations, i.e. different E and S values ($E \cong S + 1$). The figure demonstrates that the validity of an estimate of regional fault-related extension, made by summing fault displacements on a map or section showing a limited range of fault sizes, decreases with increase in the S value of the fault displacement population. For characteristic dead fault populations with S values of 0.6 and 1.0, corresponding to E values of 1.6 and 2.0, and fault displacements in the range 0.001 m–1 km, displacements greater than 100 m will account for 77 and 23%, respectively, of the fault-related extension (Fig. 7). The choice of 0.001 m as the minimum fault size is arbitrary. Particulate materials retain bulk material properties on scales down to *ca* 10 times the grain size (P. Meredith personal communication 1988) and this would represent the minimum size for a fault formed by the same physical process as larger

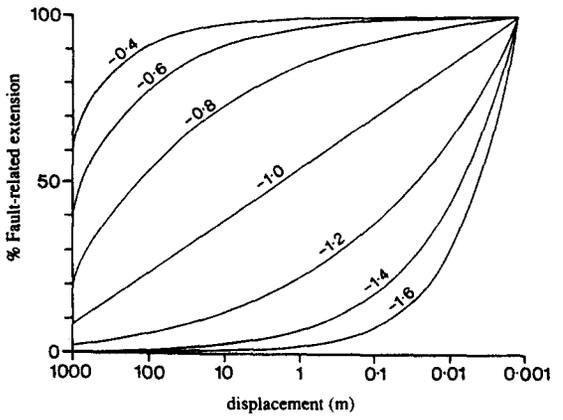

Fig. 7. Plots of displacement range vs percentage (%) fault-related extension for dead fault populations with different displacement population slopes ($-S$) and with displacements ranging from 1 mm to 1000 m. Percentage of fault-related extension accommodated by a range of displacements for a given S value can be obtained from the ordinate intersection. The diagram is valid only for populations with 1 km maximum displacement on the largest fault.

faults. Kakimi (1980) has previously recognized the significant contribution of small faults to bulk deformation from a study of minor fault populations in the South Kanto District, Japan, and presented a qualitative model for the growth of fault populations, in which successive fault populations (including active and inactive faults) are systematic but in which the E value decreases with time. Our analysis however suggests that E values reach a steady-state value after only *ca* 40 seismic cycles.

Following Strategy A, when $E = 2.0$, $S = ca\ 1.0$ and $b > 1.3$ (Table 2), a value which is outside the normal range of b values for regional seismicity. Nevertheless S values as high as 1.0 have been measured on fault populations in individual oilfields which may, however, have populations not representative of regional populations. E and S values for local regions may differ significantly from the regional values and would also be different for populations of small faults and fault displacements which are influenced by lithological variations. High population slopes appear to be characteristic of structurally complex areas, such as fault relay zones across which large displacements are transferred from one bounding fault to another. Spatial variations in b values for earthquake populations have also been described (Hirata 1989b). Recent laboratory investigations of fracture-related seismicity provide support for spatial and temporal variations in earthquake populations and this work may provide useful constraints for the future development of models for dead fault populations (Main *et al.* 1990).

The spatial distributions of faults may have an effect on estimates of regional extension. If smaller faults are clustered around larger faults, as is often the case (Hirata 1989a, Velde *et al.* 1990), then the displacements measured on larger faults may also include displacements on closely adjacent smaller faults. This effect would be expected particularly with datasets derived from seismic reflection profiles, for which the lateral resolution is limited by the survey parameters. A marked clustering effect would produce more accurate estimates of extension but would also degrade the power law fault displacement populations. We have not identified degradation of this type in the datasets examined.

For dead fault populations with low E values (*ca* 1.6 or less), the simplest explanation of discrepant extension estimates is that a significant proportion of extension is accommodated by mechanisms other than faulting (Barnett *et al.* 1987). A similar conclusion is indicated in an increasing number of tectonic terrains in which the rate of seismic energy release is reported to be a small fraction of that necessary to accommodate the bulk strain rate, calculated from plate motions, by seismic faulting (Jackson & McKenzie 1988, Solomon *et al.* 1988). Estimates of the contribution of seismic faulting to regional strain in a variety of neotectonic regions range from *ca* 100 to 10%. A shortfall in the strain rate contribution of seismic faulting can be accommodated by aseismic deformation processes, such as aseismic fault creep and plastic strain. Aseismic creep on faults

should have no effect on the relative contributions of small and large faults to regional strain or to measured fault populations. Geological and seismological studies clearly demonstrate that plastic strains, both homogeneous and heterogeneous, e.g. folds, accommodate a significant proportion of the bulk strain in compressional regimes (Cooper & Trayner 1986). Plastic strains may also accommodate a proportion of the bulk strain in extensional regimes, but associated structures will be difficult to identify because these regional plastic strains are likely to be so small as to be overshadowed even by compactional strains.

In a lithologically uniform crust the amount of stretch accommodated by seismic faulting will decrease with depth and the brittle–ductile transition effectively spans a high proportion of the crustal thickness. Observed rates of release of seismic moment are therefore derived not from a uniform elastic seismogenic layer but from a seismogenic layer with marked vertical variation in rheological properties. Pronounced lithological layering, as where a sedimentary basin overlies basement, further complicates the relationship between recorded seismic moment and stretch. Although, for convenience, we have used the concept of the seismic cycle for calculation of populations and seismic moment, this does not restrict application of the results to earthquake generating faults. For many purposes there is no significant difference between a fault on which slip and energy release occupy a few seconds every 2000 years and a fault in which the same slip and energy release are accomplished by stable sliding—the time-averaged characteristics are the same. Earthquake faulting provides the useful data because the coseismic slip and energy release are both measurable.

CONCLUSIONS

(1) Populations of dead faults have a fractal size distribution. One-dimensional sampling of fault displacements produces population slopes ($-S$) of -0.45 to -0.95 over a wide range of scales of displacement. Earthquake populations are also fractal over a wide range of magnitudes.

(2) The relationship between populations of active fractures and earthquake populations is uncertain. If the characteristic earthquake model is valid then the slopes, and fractal dimensions, of the two populations are identical.

(3) Slopes of numerically-derived populations of dead faults ($-E$) and of fault displacements ($-S$) are simply related, with $E = S + 1$.

(4) Data-derived and numerically-derived values for E, assuming the characteristic earthquake model, are compatible but require unacceptable increases in rates of seismic moment.

(5) Numerically-derived values of E for a constant seismic moment model are significantly higher than values of E derived from data.

(6) The discrepancy between the numerically-derived E values and those derived from data suggest that the fractal dimensions of active fracture populations are significantly lower than those of earthquake populations.

(7) The population differences between earthquakes and active fractures is likely to be due either to shorter recurrence intervals of earthquake events on small fractures, or to departures from the characteristic earthquake model, or to a combination of the two.

(8) No simple law has yet been found to describe the successive active fault populations which could give rise to the dead fault population data.

(9) The relative contribution of different size ranges of faults to a regional strain will vary with the E value of the dead fault population. For dead populations with fault sizes from 1 mm to 1 km and which conform with the displacement population data, as little as 17% of the strain may be accounted for by faults with displacements greater than 100 m.

Acknowledgements—We thank Conrad Childs and Chris Lavers for their assistance in compiling and plotting data and we are grateful for the discussions, help and advice of Graham Yielding of Badley Ashton & Associates. The work was funded by the British Coal Corporation and the European Coal and Steel Commission (Contract YCE.30/20214), Liverpool University Research Development Fund and the Liverpool Fault Analysis Group. The views expressed are those of the authors and not necessarily those of British Coal. We are grateful for access to data owned by oil companies in Norway and in the U.K.

REFERENCES

Angelier, J. & Colletta, B. 1983. Tension fractures and extensional tectonics. *Nature* **301**, 49–51.

Badley, M. E., Price, J. D., Rambech Dahl, C. & Agdestein, T. 1988. The structural evolution of the northern Viking Graben and its bearing upon extensional modes of basin formation. *J. geol. Soc. Lond.* **145**, 455–472.

Barnett, J. A. M., Mortimer, J., Rippon, J. H., Walsh, J. J. & Watterson, J. 1987. Displacement geometry in the volume containing a single normal fault. *Bull. Am. Ass. Petrol. Geol.* **71**, 925–937.

Barton, P. & Wood, R. 1983. Crustal thinning and subsidence in the North Sea: reply to matters arising by P. A. Ziegler. *Nature* **304**, 561.

Barton, P. & Wood, R. 1984. Tectonic evolution of the North Sea basin: crustal stretching and subsidence. *Geophys. J. R. astr. Soc.* **79**, 987–1022.

Childs, C., Walsh, J. J. & Watterson, J. 1990. A method for estimation of the density of fault displacements below the limit of seismic resolution in reservoir formations. In: *North Sea Oil and Gas Reservoirs II* (edited by The Norwegian Institute of Technology). Graham & Trotman, London, 309–318.

Cooper, M. A. & Trayner, P. M. 1986. Thrust-surface geometry: implications for thrust-belt evolution and section-balancing techniques. *J. Struct. Geol.* **8**, 305–312.

Gutenberg, B. & Richter, C. F. 1954. *Seismicity of the Earth and Associated Phenomena* (2nd edn). Princeton University Press, Princeton, New Jersey.

Hanks, T. C. & Boore, D. M. 1984. Moment–magnitude relations in theory and practice. *J. geophys. Res.* **89**, 6229–6235.

Heffer, K. & Bevan, T. 1990. Scaling relationships in natural fractures—data, theory and applications. *Proc. European Petrol. Conf.* **2**, 367–376 (SPE paper No. 20981).

Hellinger, S. J. & Sclater, J. 1983. Some comments on two-layer extensional models for the evolution of sedimentary basins. *J. geophys. Res.* **88**, 8251–8269.

Hirata, T. 1989a. Fractal dimension of fault systems in Japan: fractal study in rock fracture geometry at various scales. *Pure & Appl. Geophys.* **131**, 157–170.

Hirata, T. 1989b. A correlation between the *b* value and the fractal dimension of earthquakes. *J. geophys. Res.* **94**, 7507–7514.
Huang, J. & Turcotte, D. L. 1990. Evidence for chaotic fault interactions in the seismicity of the San Andreas fault and Nankai trough. *Nature* **348**, 234–236.
Jackson, J. A. & McKenzie, D. 1988. The relationship between plate motions and seismic tensors, and the rates of active deformation in the Mediterranean and Middle East. *Geophys. J.* **93**, 45–73.
Kakimi, T. 1980. Magnitude–frequency relation for displacement of minor faults and its significance in crustal deformation. *Bull. geol. Surv. Jap.* **31**, 467–487.
Kanamori, H. & Anderson, D. 1975. Theoretical basis for some empirical relations in seismology. *Bull. seism. Soc. Am.* **65**, 1073–1085.
King, G. 1983. The accommodation of large strains in the upper lithosphere of the earth and other solids by self-similar fault systems: the geometrical origin of *b*-value. *Pure & Appl. Geophys.* **5/6**, 761–815.
Kostrov, V. V. 1974. Seismic moment and energy of earthquakes, and seismic flow of rocks. *Izvestia Earth Physics* **1**, 13–21.
Kusznir, N. J., Al-Saigh, N. H. & Ashwin, D. P. 1984. Induced seismicity generated by longwall coal mining in the North Staffordshire coal-field, U.K. In: *Proc. 1st Int. Congr. on Rockbursts and Seismicity in Mines*, Johannesburg, 1982 (edited by Gay, N. C. & Wainwright, E. H.). South African Institute of Mining and Metallurgy, Johannesburg.
Main, I. G., Meredith, P. G., Sammonds, P. R. & Jones, C. 1990. Influence of fractal flaw distributions on rock deformation in the brittle field. In: *Deformation Mechanisms, Rheology and Tectonics* (edited by Knipe, R. J. & Rutter, E. H.). *Spec. Publs geol. Soc. Lond.* **54**, 81–96.
Marrett, R. & Allmendinger, R. W. 1990. Kinematic analysis of fault-slip data. *J. Struct. Geol.* **12**, 973–986.
Marrett, R. & Allmendinger, R. W. 1991. Estimates of strain due to brittle faulting: sampling of fault populations. *J. Struct. Geol.* **13**, 735–737.
McKenzie, D. P. 1978. Some remarks on the development of sedimentary basins. *Earth Planet. Sci. Lett.* **40**, 25–32.
Mogi, K. 1962. Magnitude frequency relation for elastic shocks caused by the fracture of heterogeneous materials and its relation to earthquake phenomena. *Bull. Earthquake Res. Inst. Tokyo Univ.* **40**, 125–173.
Royden, L. & Keen, C. E. 1980. Rifting process and thermal evolution of the continental margin of eastern Canada determined from subsidence curves. *Earth Planet. Sci. Lett.* **51**, 343–361.
Sassi, W., Livera, S. E. & Caline, B. P. R. In press. Quantification of the impact of subseismic scale faults in Cormorant Block IV, UK Northern North Sea. In: *Structural and Tectonic Modelling and its Application to Petroleum Geology* (edited by Norsk Petroleumsforening). Graham & Trotman, London.
Scholz, C. H. 1968. The frequency magnitude relation of microfracturing in rock and its relation to earthquakes. *Bull. seism. Soc. Am.* **58**, 399–415.
Scholz, C. H. 1982. Scaling laws for large earthquakes: consequences for physical models. *Bull. seism. Soc. Am.* **72**, 1–14.
Scholz, C. H. 1990. Earthquakes as chaos. *Nature* **348**, 197–198.
Scholz, C. H., Aviles, C. A. & Wesnousky, S. G. 1986. Scaling differences between large interplate and intraplate earthquakes. *Bull. seism. Soc. Am.* **76**, 65–70.
Scholz, C. H. & Cowie, P. A. 1990. Determination of geologic strain from fault slip data. *Nature* **346**, 837–839.
Schwartz, D. P. & Coppersmith, K. J. 1984. Fault behaviour and characteristic earthquakes: Examples from the Wasatch and San Andreas fault zones. *J. geophys. Res.* **89**, 5681–5698.
Schwartz, D. P., Coppersmith, K. J., Swan, F. H., Somerville, P. & Savage, W. U. 1981. Characteristic earthquakes on intraplate normal faults (Abs.). *Earthquake Notes* **52**, 71.
Solomon, S. C., Huang, P. Y. & Meinke, L. 1988. The seismic moment budget of slowly spreading ridges. *Nature* **334**, 58–60.
Turcotte, D. L. 1986. A fractal model for crustal deformation. *Tectonophysics* **132**, 261–269.
Velde, B., Dubois, J., Touchard, G. & Badri, A. 1990. Fractal analysis of fractures in rocks: the Cantor's Dust method. *Tectonophysics* **179**, 345–352.
Villemin, T. & Sunwoo, C. 1987. Distribution logarithmique self-similaire des rejets et longeurs de failles: exemple du bassin houlier Lorrain. *C. r. Acad. Sci., Paris* **305**, 1309–1312.
Walsh, J. J. & Watterson, J. 1987. Distributions of cumulative displacement and seismic slip on a single normal fault surface. *J. Struct. Geol.* **9**, 1039–1046.
Walsh, J. J. & Watterson, J. 1988. Analysis of the relationship between displacements and dimensions of faults. *J. Struct. Geol.* **10**, 239–247.
Walsh, J. J. & Watterson, J. 1989. Displacement gradients on fault surfaces. *J. Struct. Geol.* **11**, 307–316.
Walsh, J. J. & Watterson, J. 1990. New methods of fault projection for coalmine planning. *Proc. Yorks. geol. Soc.* **48**, 209–219.
Walsh, J. J. & Watterson, J. 1991. Geometric and kinematic coherence and scale effects in normal fault systems. In: *Geometry of Normal Faults* (edited by Roberts, A., Yielding, G. & Freeman, B.). *Spec. Publs geol. Soc. Lond.* **56**, 193–203.
Walsh, J. J., Watterson, J. & Yielding, G. 1991. The importance of small scale faulting in regional extension. *Nature* **351**, 391–393.
Watterson, J. 1986. Fault dimensions, displacements and growth. *Pure & Appl. Geophys.* **124**, 365–373.
Wesnousky, S. G., Scholz, C. H., Shimazaki, K. & Matsuda, T. 1983. Earthquake frequency distribution and mechanics of faulting. *J. geophys. Res.* **88**, 9331–9340.
White, N. J., Jackson, J. A. & McKenzie, D. P. 1986. The relationship between the geometry of normal faults and that of the sedimentary layers in their hanging walls. *J. Struct. Geol.* **8**, 897–901.
White, N. 1987. Constraints on the measurement of extension in the brittle upper crust. *Norsk geol. Tidsskr.* **67**, 269–279.

APPENDIX 1

CALCULATION OF DEAD FAULT POPULATIONS

Strategy A

The attributes of an active fault population satisfying the G–R relationship are shown in Table 1. The slip increment on each fault increases by 1 mm with each cycle and, if $D/W^2 = 10^{-6}$ (Walsh & Watterson 1988), the width of each fault increases by 31.62 m with each cycle. The number of events (z_i) required for the smallest faults of one class to grow to the size of the next class is shown. For calculation purposes it is more convenient to define size class boundaries so that for a given number of slip events the smallest faults of one class will grow to the minimum size of the next class; it is also necessary to use more size classes than in the simple case shown in Table 1.

A fault with current maximum displacement D_0, and slip u_0, will grow as follows.

After one further slip event,

$$D_1 = D_0 + (u_0 + e),$$

where D_1 = maximum displacement and e = increment of slip increase.

After two events,

$$D_2 = D_0 + (u_0 + e) + (u_0 + 2e).$$

After three events,

$$D_3 = D_0 + (u_0 + e) + (u_0 + 2e) + (u_0 + 3e).$$

After i events,

$$D_i = D_0 + (u_0 i) + ei(i + 1)/2. \quad \text{(A1)}$$

If $D = cW^2$ and $u/W = k$ then

$$W = (D/c)^{1/2}$$

$$u = kW$$

$$u = k(D/c)^{1/2}. \quad \text{(A2)}$$

Combining (A1) and (A2)

$$D_i = D_0 + ik(D_0/c)^{1/2} + (ei(i + 1))/2. \quad \text{(A3)}$$

The ranges of values of k, c and e are known (Walsh & Watterson 1988) and each value can be varied, within these ranges, in the following calculations. For a selected value of i, a series of values of D can be calculated representing the boundaries of classes for which faults will grow to the next class size after i events. 1000 classes (0–999) are defined, bounded by maximum displacements D_0, D_1, D_2 D_3, ..., D_{1000}. D_0 is set at 0.001 m but can be varied.

For an initial active fault population conforming to the G–R relationship (with a selected b value) and characterized by the size of the largest fault present, the numbers of faults in each class are calculated.

One cycle of i events increases the number of faults in a class to the size of the next class, thus increasing the largest fault in the population by one class. After each cycle the number of faults in each class is provisionally transferred to the next highest class. On the basis of the new largest fault size, the numbers required in each class to maintain a G–R relationship are recalculated. Too many have been provisionally transferred to each class from the next class down, so the number of excess faults in each class is calculated and transferred back to the next smaller class, and summed as inactive faults. After a chosen number of iterations of i events the current active population is added to the inactive population in each size class to obtain the total population of faults existing at the end of the tectonic event, i.e. the dead fault population.

Strategy B

The growth law for individual faults is the same as for Strategy A. The initial fault population is defined by the chosen number of faults in the smallest size class; size classes are separated by one increment of slip. The total seismic moment of all these faults, ΣM_0, is calculated and is equivalent to the rate of seismic moment, $\Sigma \dot{M}_0$, if the recurrence interval is constant. After each seismic cycle, or slip increment, the numbers of faults are calculated to satisfy two conditions: (i) that the G–R relationship is maintained, and (ii) the new population of active faults has the same value of ΣM_0 as preceding active populations. After each seismic cycle faults in excess of those required for the active population are consigned to the accumulating inactive fault population. After a chosen number of cycles the current active population is added to the inactive population to give the dead fault population.

APPENDIX 2

DERIVING THE LIFETIME SEISMIC MOMENT

The lifetime seismic moment (M_{0L}) of a fault is derived as follows.

$M_0 = mu\mu W^2$ for a circular fault, where M_0 = seismic moment for a single event, u = slip in a single event, W = fault dimension and μ = shear modulus.

For a fault grown in i increments

$$M_{0L} = im\underline{u}\mu\underline{W}^2,$$

where $\underline{W}^2$ = mean W^2 for all slip events in the lifetime of a fault and $\underline{u}$ = mean slip for all slip events.

Successive values of W are $W_1, W_2, W_3, \ldots, W_i$, where $W_{n+1} - W_n$ = constant and successive values of W constitute an arithmetic series with small or zero first term:

$$\Sigma[W_1^2 + W_2^2 + W_3^2 \ldots + W_i^2] = (W_i + 0.5)^3/3 = W_i^3/3,$$

when i is large, so

$$\underline{W}^2 = W_i^3/3i.$$

Successive values of u ($u_1, u_2, u_3, \ldots, u_i$) constitute an arithmetic series so

$$\underline{u} = u_i/2$$

and

$$M_{0L} = i\mu(u_i/2)(W_i^3/3i)$$

as

$$u_i/W_i = k \qquad (\text{where } k = 3.6 \times 10^{-5})$$
$$u_i = kW_i$$

so

$$M_{0L} = (\mu\pi k W^4)/6$$

as

$$D_i = cW_i^2$$
$$W_i = (D_i/c)^{1/2}$$
$$M_{0L} = (\mu\pi k((D_i/c)^{1/2})^4)/6$$
$$M_{0L} = D_i^2/c^2 \cdot \text{constant}$$
$$M_{0L} = D_i^2 \cdot \text{constant}$$

or, for a single fault,

$$\log M_{0L} = 2 \log D + \text{constant}$$

for a dead fault population where

$$\log N = a - E \log D$$
$$\log D \propto (1/E) \log N.$$

If ΣM_{0L} = aggregate lifetime seismic moments of faults with cumulative number N and largest fault of maximum displacement D then

$$\log \Sigma M_{0L} \propto (2 \log N)/E.$$

Convergence of $\log \Sigma M_{0L}$ to a finite value does not require $E < 1$.